Available online at www.sciencedirect.com
ScienceDirect
Journal of Organometallic Chemistry 692 (2007) 2669–2677
Journal of Organometallic Chemistry
www.elsevier.com/locate/jorganchem

Novel inorganic rings and materials deposition

Chinh Q. Nguyen, Mohammad Afzaal, Mohammad A. Malik, Madeleine Helliwell, Jim Raftery, Paul O'Brien *

The School of Chemistry and the School of Materials, The University of Manchester, Oxford Road, Manchester M13 9PL, UK

Received 20 October 2006; received in revised form 24 November 2006; accepted 24 November 2006
Available online 5 December 2006

Abstract

This paper discusses the use of two relative unexploited classes of molecules based on imino-dialkylphosphinate [$(EPR_2)_2NH$] (E = Se or Te) and dialkyldiselenophosphinate [$HNEt_3$][R_2PSe_2] and subsequently, their potential for the deposition of useful materials as either thin films or nanoparticles. The structural properties of the materials obtained were elucidated by means of X-ray powder diffraction, scanning electron microscope and transmission electron microscope.

Keywords: Chalcogenide; Selenophosphinate; Chemical vapor deposition; Nanoparticles

1. Introduction

During the past decade, considerable attention has been directed towards the investigation of single-source precursors (SSPs) for semiconductors, as thin films, or in nanoparticlulate form. Conventional metal-organic chemical vapour deposition (MOCVD) uses as many elemental sources as there are component elements in the material. Multiple-source routes often use highly toxic and/or oxygen or moisture sensitive gases, or very volatile ligands, such as: $(CH_3)_2Zn$ $(Et_3)_3Ga$, H_2E (E = S or Se) or EH_3(E = N, P or As). Environmental and safety conditions are ever increasing concerns for industrial processes and various specific benefits are expected from SSPs. Potentially, using one molecule instead of several results in simplified delivery of materials to the reaction zone. In many cases, SSPs provide a safer route by being intrinsically easier to handle. We have been interested in chalcogenide containing precursors particularly for sulfides, selenides or tellurides as thin films or as nanoparticles. For example, it has been demonstrated that selenocarbamates such as [M^n(SeCNRR')$_n$] are suitable for the synthesis of many group 12 chalcogenides [1,2]. However, the diselenocarbamato ligand is prepared from toxic and noxious carbon diselenide.

In order to find alternative chalcogenide sources, studies were carried on diselenophosphinates and ditelluroimidodiphosphinates. The coordination chemistry of dithiophosphinato complexes has been well described [3]. The examples of fully characterised selenophosphinates are rare. However, there is some recent work on the coordination chemistry of diselenophosphates or diselenophosphonates [4]. The original methods for the preparation of diselenophosphates or diselenophosphinates were based on reactions between Na_xE_y (E = S, Se, Te) and $Ph_2P(Se)Cl$ [5]. The synthesis of Na_xE_y involves the reaction between sodium metal and selenium in liquid ammonia (−78 °C). It was reported by Woollins and co-workers that such reactions give a mixture of products as well as un-reacted sodium metal, and authors have suggested that the reaction between Na_xE_y and $Ph_2P(Se)Cl$ is irreproducible [6]. However, they did report the X-ray single crystal structure of $[Na_2(Se_2PPh_2)_2{\cdot}THF{\cdot}5H_2O]$ [6] and of $[K_2(PhPSe_2)_2CH_2]$ [7]. Other notable examples of metal selenophosphinates include $[Ph_2PSe_2Li \cdot THF \cdot TMEDA]$ [TMEDA = $\{(CH_3)_2NCH_2\}_2$] [8] and $[K(Se_2PPh_2)(THF)_2]_2$ [9]. The indium complex;

* Corresponding author.
E-mail address: paul.obrien@manchester.ac.uk (P. O'Brien).

0022-328X/$ - see front matter © 2006 Elsevier B.V. All rights reserved.
doi:10.1016/j.jorganchem.2006.11.043

$[In(Se_2PPh_2)_3]$ was prepared in situ by the reaction of the $InCl_3$ and $[K(Se_2PPh_2)(THF)_2]_2$ [9]. The selenophosphinates reported are unstable and highly air sensitive and their preparations involve difficult reaction conditions. More recently, we have reported a facile route for the preparation of $[(R_2PSe)_2Se]$ (R = Ph, ^{i}Pr) in ca. 45% yield [10]. Further investigations on diselenophosphinate ligands have led to the isolation of the $(R_2PSe_2)^-$ anion crystallised as an alkylammonium salt in the form of $[HNEt_3][R_2PSe_2]$ (R = ^{i}Pr (**1**), ^{t}Bu (**2**), Ph (**3**)). In the first part of the paper, we will report the synthesis and characterisation of the isolated ligands.

Imidodiphosphinic acid derivatives $R_2P(E)NH(E)PR'_2$ (R, R′ = CH_3, C_6H_5; E = O, S, NH) were first prepared by Schmidpeter [11]. The synthesis process was improved by Woollins and co-workers to make a wider range of derivatives with R, R′ = ^{i}Pr, ^{t}Bu, Et, OEt, OPh and E = S, Se [12–16],[17],[18,19]. On deprotonation of the amine, the $R_2P(E)NH(E)PR_2$ molecule becomes a bidentate chelating ligand analogous to acetylacetonate (acac or 2,4 pentanedionato) type. The ligand can form neutral complexes of the type $[M(N(R_2PE)_2)_n]$ with many transition or main group metals. The selenium analogue have been successfully used for the deposition of semiconductor thin films and nanoparticulate preparation [20–24]. The tellurium analogue of $R_2P(E)NH(E)PR_2$ could not be prepared by oxidizing R_2PNHPR_2 with telurium [25]. Recently Chivers and co-workers have developed a new route, in which R_2PNHPR_2 first metalated by NaH to form $Na[R_2PNPR_2]$ was reacted with tellurium powder in hot toluene in the presence of *N*,*N*,*N*′,*N*′-tetramethylethylenediamine (TMEDA) [26–28]. A range of metal complexes $M[N(PPr^i_2Te)_2]_n$ (M = Zn, Cd, Hg, Sb, Bi; *n* = 2 or 3) were produced when the metal halide was reacted with $Na[N(TePPr^i_2)_2]$ [29].

Nano-wires, -rods, and other nanodimensional materials have been intensively researched in recent years because of their unique properties [30]. Quantum confinement effects come into play and affect, most notably, the electronic properties when the length is in nanometers. A key step in the advancement of nanoscience is devising synthetic strategies to yield nanodimensional matter with good control over shape and size. Nanorods and nanowires of metals, chalcogenides, and oxides have been obtained by different methods [31]. Many of these methods rely on templates such as porous alumina to direct growth. Relative little progress has been made on the controlled synthesis of 1D nanostructures of ZnSe. A number of techniques based on physical and chemical approaches have been used to synthesis ZnSe nanowires ~10–100 nm wide and lengths of up to few microns [32]. However, the dimensions of the particles are larger than the Bohr radius (4.5 nm), [33] and any quantum confinement effects are expected to be very limited. Recently, Panda and co-workers have reported a facile synthesis of ZnSe nanorods and nanowires which exhibit quantum confinement properties [34]. Reports of ZnSe nanostructures synthesised from single-source precursors (SSPs) are scarce due to lack of suitable selenium containing ligands [35,36]. Building on our experience with solution-phase synthesis of semiconductor nanocrystalline materials, we have developed simple synthetic routes to semiconductor nanorods. In the second part, we report the synthesis and characterisation of ZnSe nanorods from $[Zn(^iPr_2PSe_2)_2]$.

In the final part of this paper, deposition of antimony telluride (Sb_2Te_3), a narrow band gap, layered semiconductor widely used in thermoelectric generators and coolers, is carried out using $Sb[(TeP^iPr_2)_2N]_3$. The deposition was conducted in an aerosol-assisted chemical vapour deposition (AACVD) method and the resulting materials were physically and structurally characterised.

2. Experimental

2.1. General procedures

All the reactions were performed under an atmosphere of nitrogen using standard Schlenk techniques. All chemicals were bought from Aldrich Chemical Company Limited and used as received. Solvents were distilled prior to use.

2.2. Analytical techniques

NMR spectra were obtained on chloroform-D_6 solution using a Bruker AC300 FTNMR instrument. Element analysis was performed by the University of Manchester microanalytical laboratory. The mass spectra were carried out in atmospheric pressure chemical ionization (APCI) mode. The X-ray powder diffraction (XRPD) studies were carried out by a Bruker AXS D8 diffractometer using monochromated Cu K_α radiation. The samples were prepared by dropping suspensions of nanopartilces in hexane onto glass substrates and leaving to dry. The substrates were mounted flat and scanned with a step size of 0.01° and a count rate of 1.2 s. The diffraction patterns were then compared to the documented patterns in the joint committee on powder diffraction standards (JCPDS) index. Transmission electron microscopy (TEM) was employed to characterize the morphology of nanoparticles with Philips Tecnai F30 300 kV FEG TEM. Dilute suspensions of nanoparticle samples in hexane were dropped onto TEM grids and left to dry for observation.

2.3. X-ray single crystallography

Single crystal X-ray crystallography measurements were made using graphite monochromated Mo Kα radiation on a Bruker APEX diffractometer. The structures were solved by direct methods and refined by full-matrix least-squares on F^2 [37]. All calculations were carried out using the SHELXTL package [38]. All non-hydrogen atoms were refined with anisotropic atomic displacement parameters. Hydrogen atoms were placed in calculated positions, assigned isotropic thermal parameters and allowed to ride on their

Table 1
Crystal data and structural refinement of $[HNEt_3][R_2PSe_2]$; (R = ^{i}Pr (**1**); ^{t}Bu (**2**); Ph (**3**))

Compound	**1**	**2**	**3**
Empirical formula	$C_{12}H_{30}NPSe_2$	$C_{14}H_{34}NPSe_2$	$C_{18}H_{26}NPSe_2$
Fw	377.26	405.31	445.29
Temperature (K)	100(2)	100(2)	100(2)
Wavelength (Å)	0.71073	0.71073	0.71073
Crystal system	Monoclinic	Tetragonal	Orthorhombic
Space group	*P*2(1)/c	*P*4(1)2(1)2	*Pnma*
a (Å)	7.811(4)	8.4388(4)	14.8513(16)
b (Å)	14.460(7)	8.4388(4)	13.7554(15)
c (Å)	15.403(8)	26.5562(19)	9.4189(10)
α (°)	90	90	90
β (°)	99.374(9)	90	90
γ (°)	90	90	90
Volume (Å^3)	1716.5(15)	1891.16(19)	1924.1(4)
Z	4	4	4
d_{calc} (mg/m^3)	1.460	1.424	1.537
Absolute coefficient (mm^{-1})	4.383	3.983	3.923
F (000)	768	832	896
Crystal size	0.25 × 0.20 × 0.15	0.50 × 0.40 × 0.30	0.35 × 0.20 × 0.08
Index ranges	$-10 \leqslant h \leqslant 9$, $-19 \leqslant k \leqslant 19$, $-19 \leqslant l \leqslant 19$	$-10 \leqslant h \leqslant 10$, $-10 \leqslant k \leqslant 10$, $-33 \leqslant l \leqslant 32$	$-17 \leqslant h \leqslant 18$ $-17 \leqslant k \leqslant 11$, $-9 \leqslant l \leqslant 11$
Collected/unique	14664/4076	15059/1948	10596/2059
R_{int}	0.0982	0.0343	0.0293
Data/restraints/pars.	4076/0/143	1948/57/122	2059/0/113
Goodness-of-fit on F^2	0.770	0.730	1.051
R_1, wR_2 [$I > 2\sigma(I)$]	0.0362, 0.0610	0.0411, 0.1056	0.0236, 0.0576
R_1, wR_2 (all data)	0.0581, 0.0654	0.0426, 0.1077	0.0265, 0.0588
Different peak, hole (e Å)	0.745, −0.532	0.622, −1.048	0.652, −0.256

parent carbon atoms. Crystallographic details and selected interatomic distances and angles are summarised in Tables 1 and 2.

2.4. Synthesis of $[HNEt_3][^iPr_2PSe_2]$ (*1*)

^{i}Pr$_2$PCl (4.8 mL, 30 mmol) and $HSiEt_3$ (9.6 mL, 60 mmol) were dissolved in 150 mL cold dry toluene under nitrogen followed by NEt_3 (8.3 mL, 60 mmol). The mixture was stirred at room temperature for 6 h forming a white cloudy precipitate. Grey Se powder (4.7 g, 60 mmol) was added to the solution and refluxed for 20 h, leading to a dark red solution and white precipitate. The white precipitate was filtered off. The resulting solution was reduced to ~50 mL and kept at 0 °C to produce yellow crystals. The crystals were filtered and washed with cold hexane. Yield (10 g, yield 89%). Elemental Anal. calc. (%) for $C_{12}H_{30}NPSe_2$: C, 38.20; H, 8.02; N, 3.71; P, 8.21. Found: C, 38.66; H, 8.13; N, 3.59; P 8.37%. ^{13}C NMR $\delta = 8.72$ ppm (CH_3, Et), 17.77 ppm (CH_3, ^{i}Pr), 33.65 ppm & 34.14 ppm (CH, ^{i}Pr), 45.97 ppm (CH_2, Et); ^{1}H NMR $\delta = 3.21$ ppm (q, 6H, CH_2, Et, $J = 7.3$ Hz), 2.14 ppm (dd, 2H, CH, ^{i}Pr, $J = 6.4$ Hz, $J = 13.3$ Hz), 1.33 ppm (t, 9H, CH_3,Et, $J = 7.3$ Hz), 1.18 ppm (dd, 12H, CH_3, ^{i}Pr, $J = 6.3$ Hz, $J = 19.1$ Hz). ^{31}P NMR (162 MHz): $\delta = 64.9$ ppm (s + d satellites, $^1J_{PSe} = 574$ Hz). MS: $(HNEt_3)^+ = 102$, $(^iPr_2PSe_2)^- = 275$.

2.5. Synthesis of $[HNEt_3][^tBu_2PSe_2]$ (*2*)

The compound was prepared in a similar way to **1** but used ^{t}Bu$_2$PCl (5.7 mL, 30 mmol) to obtain yellow crystals of **2** (9.6 g, yield 80%). Elemental Anal. calc. (%) for

Table 2
Selected bond distances (Å) and angles (°) for $(HNEt_3)(R_2PSe_2)$ (R = ^{i}Pr (**1**); ^{t}Bu (**2**); Ph (**3**))

Compounds	Bond distances (Å)		Bond angles (°)	
1	C(1)–P(1)	1.845(3)	C(1)–P(1)–C(4)	105.31(1)
	C(4)–P(1)	1.846(3)	C(1)–P(1)–Se(2)	109.03(1)
	P(1)–Se(2)	2.1520	C(4)–P(1)–Se(2)	108.22(1)
	P(1)–Se(1)	2.1716	C(1)–P(1)–Se(1)	107.88(1)
			C(4)–P(1)–Se(1)	108.14(1)
			Se(2)–P(1)–Se(1)	117.6
2	Se(1)–P(2)	2.162(1)	C(1)–P(2)–C(1A)	112.4(3)
	P(2)–C(1)	1.888(4)	C(1)–P(2)–Se(1A)	108.49(4)
	P(2)–C(1A)	1.888(4)	C(1A)–P(2)–Se(1A)	106.58(2)
	P(2)–Se(1A)	2.1620(1)	C(1)–P(2)–Se(1)	106.58(2)
			C(1A)–P(2)–Se(1)	108.49(1)
			Se(1A)–P(2)–Se(1)	114.39(8)
3	Se(1)–P(1)	2.159(8)	C(1A)–P(1)–C(1)	102.39(1)
	Se(2)–P(1)	2.139(7)	C(1A)–P(1)–Se(2)	110.48(6)
	P(1)–C(1A)	1.835(2)	C(1)–P(1)–Se(2)	110.48(6)
	P(1)–C(1)	1.835(2)	C(1A)–P(1)–Se(1)	107.83(6)
			C(1)–P(1)–Se(1)	107.83(6)
			Se(2)–P(1)–Se(1)	116.81(3)

$C_{14}H_{34}NPSe_2$: C, 41.49; H, 8.46; N, 3.46; P, 7.64. Found: C, 41.53; H, 8.71; N, 3.47; P, 7.57%. ^{13}C NMR $\delta = 45.84$ ppm (CH_2, Et), 40.98, 40.63 ppm (CH, t–Bu), 28.75 ppm (CH_3, Et), 8.64 ppm (CH_3, t-Bu). 1H NMR $\delta = 1.3$ ppm (t, CH_3, Et, $J = 7.3$ Hz), 1.4 ppm (d, CH_3, t–Bu, $J = 16.4$ Hz), 3.3 ppm (q, CH_2, Et, $J = 7.3$ Hz). ^{31}P NMR (162 MHz): $\delta = 92.3$ ppm (s + d satellites, $^1JPSe = 567.2$ Hz). MS: $[(^tBu)_2PSe_2]^- = 302$.

2.6. Synthesis of $[HNEt_3][Ph_2PSe_2]$ (3)

The compound was prepared in a similar way to **1** but used $(Ph)_2PCl$ (5.9 mL, 30 mmol) to obtain yellow crystals of **3**. (13.36 g, yield 85%). Elemental Anal. calc. (%) for $C_{18}H_{26}NPSe_2$: C, 48.55; H, 5.89; N, 3.15; P, 6.96. Found: C, 48.41; H, 5.95; N, 3.18; P 6.88%. ^{13}C NMR $\delta = 8.77$ ppm (CH_3, Et), 46.20 ppm (CH_2, Et); 127.68, 127.85, 129.70, 131.37, 131.52 (Ph). ^1H NMR $\delta = 8.13$ ppm (dd, Ph, $J = 7.0$ Hz, $J = 14.1$ Hz); 7.31 ppm (d, Ph, $J = 2.9$ Hz); 7.29 ppm (d, Ph, $J = 2.6$ Hz); 3.26 ppm (q, CH2, Et, $J = 7.3$ Hz); 1.32 ppm (t, CH_3, Et, $J = 7.3$ Hz). ^{31}P NMR (162 MHz): $\delta = 20.5$ ppm (s + d satellites, $^1JPSe = 602$ Hz). MS: $(HNEt_3)^+ = 102$, $(Ph_2PSe_2)^- = 343$.

2.7. Synthesis of $[Zn(^iPr_2PSe_2)_2]$ (4)

Solution of $ZnCl_2$ (0.68 g, 5 mmol) in 5 ml H_2O was added drop wise to solution of $[HNEt_3][^iPr_2PSe_2]$ (3.77 g, 10 mmol) in 100 ml of MeOH. The mixture was stirred for 1 h at room temperature forming a yellow precipitate, which was filtered, washed with hot MeOH and re-crystallized in dichloromethane to obtain yellow crystals of **4** (2.27 g, 73.6%), m.p. 120 °C. Elemental Anal. Calc. for $C_{12}H_{28}P_2Se_4Zn$: C, 23.42; H, 4.59; P,10.06; Zn, 10.62. Found: C, 23.49; H, 4.46; P, 10.29; Zn, 10.48%. δ_H(300 MHz; $CDCl_3$; Me_4Si) 1.25 (dd, 24H, J 6.8 and 20.7, $4 \times CH(CH_3)_2$), 2.17 (dq, 4H, $J = 6.9$ Hz, $J = 11.1$ Hz, $4 \times CH(CH_3)_2$). ^{31}P NMR (162 MHz): $\delta = 61.6$ ppm (s + d satellites, $^1J_{PSe} = 442.9$ Hz).

2.8. Growth of ZnSe nanoparticles

A solution of 0.2–0.6 g of $[Zn(^iPr_2PSe_2)_2]$ in 2 mL trioctylphosphine (TOP) was injected into 5 g hexadecylamine (HDA) at 300 °C under N_2, and the reaction was kept for 30–70 min. As the temperature of the reaction solution dropped down to 70 °C, 100 mL methanol was added to the reaction mixture, then yellowish ZnSe nanoparticles were isolated with centrifuge and washed for 2 times with methanol (100 mL each time).

3. Results and discussion

In this paper, a simple one-step method for the reproducible synthesis of dichalcogenophosphinates; $(HNEt_3)(R_2PSe_2)$ (R = ^{i}Pr (**1**), ^{t}Bu (**2**), Ph (**3**)) (Eq. (1)). The compounds were synthesized in high yield (>80%) and are of good purity. The preparation of the related neutral species $(R_2PSe)_2Se$ (R = Ph, ^{i}Pr) cannot be achieved at more than 45% yield [10].

$$R_2PCl + 2HSiEt_3 + 2NEt_3 \xrightarrow[\text{Toluene}]{\text{Se}} (R_2PSe_2)(HNEt_3) + ClHNEt_3 + Si_2Et_6 \quad (1)$$

$$R = {}^iPr; {}^tBu; Ph$$

The synthesised ionic compounds are air and moisture stable and for the first time have been fully characterized including structure determination by X-ray single crystallography. All are readily soluble in most common organic solvents. In our previous work, $HSiCl_3$ was used in the synthesis of $(R_2PSe)_2Se$ (R = Ph, ^{i}Pr) [10]. In this study, excess $HSiEt_3$ and triethylamine were used yielding the $(R_2PSe_2)^-$ species. $HSiEt_3$ was used instead of $HSiCl_3$ because $HSiCl_3$ reacts readily with NEt_3 to form $(HNEt_3)(SiCl_3)$ as a precipitate, making Se insertion difficult.

The ^1H NMR of (**1**) shows a triplet and a quartet for methyl and methylene protons of triethylammonium ion. Whereas, the isopropyl groups at phosphorus gives doublet of doublet for methyl protons and a doublet of doublet for methylene protons due to coupling with methyl protons and phosphorus. The ^{13}C NMR indicates splitting of methyl and methylene carbons of isopropyl groups which confirms non-equivalent carbons. The ^1H and ^{13}C NMR spectra of compounds (**2**) and (**3**) are as expected confirming the presence of the *tert*-butyl and phenyl moities. The ^{31}P NMR spectra of (**1**), (**2**) and (**3**) displayed sharp singlets at δ(P) 64.96, 92.3 and 20.5 ppm, respectively. In each case the singlet is accompanied by a single pair of selenium satellites with ^{31}P–^{77}Se coupling constants in the range 567–602 Hz, indicating a P–Se bond order of approximately 1.5 as expected. The mass spectra of $(R_2PSe_2)^-$ (R = ^{i}Pr, Ph) show a base peak at 275 and 343, respectively, confirming the expected compounds.

The crystals suitable for X-ray diffraction studies were obtained from a concentrated solution in methanol at low temperature. The X-ray crystal structure of (**1**) indicates that it crystallizes as an ionic salt, composed of the anion $(^iPr_2PSe_2)^-$ and the cation $(Et_3NH)^+$ (Fig. 1). The coordination geometry around phosphorus is distorted tetrahedra with bond angles ranging between 105.3(1)° and 117.6°. The phosphorus and selenium bond lengths (2.152 and 2.172 Å) within the selenophosphinite unit are intermediate between single (P–Se 2.20(8) Å) [6] and double (P=Se 2.072(2) Å) [10] bonds. These bond lengths strongly suggest a delocalization of negative charge over the PSe_2 unit. The crystal structure of (**2**) is disordered at the cation and is not shown here (Fig. 2). Nevertheless, the phosphorus and selenium bond lengths in (**2**) are also intermediate between single and double bond character. All P–Se bond lengths in (**1**) and (**2**) are similar in magnitude to those found in $[Ph_2PSe_2Li{\cdot}THF{\cdot}TMEDA]$ [8]. The reported crystal structure of $(^iPr_2PSe_2)Se$ contains discrete

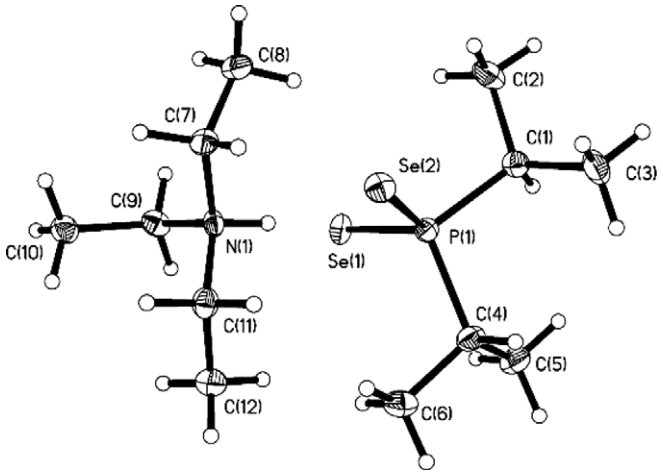

Fig. 1. Thermal ellipsoid plot (50% probability) of the structure of (**1**).

single and double bonds of phosphorus and selenium [10]. The Se–P–Se bite angle is reduced from 117.6° in (**1**) to 114.39(8)° in (**2**) as expected, simply due to more bulky alkyl group as in **(2).**

Similar to (**1**) and (**2**), compound (**3**) also adopts a monomeric structure in the solid state with a tetrahedral geometry about the phosphorus atom, and no intermolecular interactions are observed (Fig. 3). The geometry around phosphorus is highly distorted from tetrahedral, due to steric effects exerted by the phenyl groups. The P(1)–Se(2) bond length is also reduced to 2.139(7) Å which is smaller than P–Se bond lengths in (**1**). This difference may be conventionally accounted by the strong electron withdrawing behavior of the phenyl rings, as compared to the alkyl chains.

The reactions of p-block and d-block metal ions with $(HNEt_3)(R_2PSe_2)$ leads to formation of air-stable, inorganic complexes in which $(R_2PSe_2)^-$ anion acts as a chelating ligand (Fig. 4) [39].

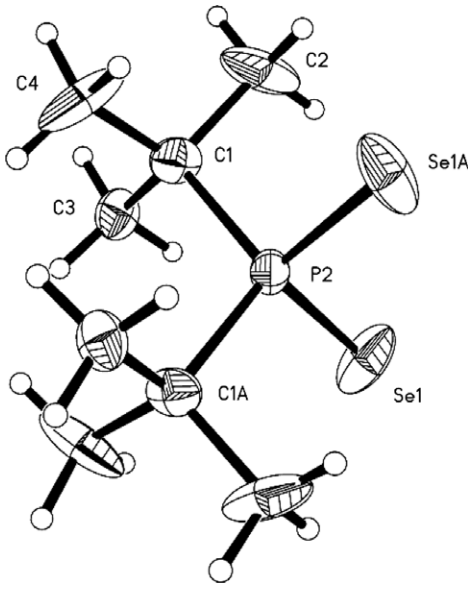

Fig. 2. Thermal ellipsoid plot (50% probability) of the structure of (**2**). The crystal structure is disordered at the cation and is not shown here.

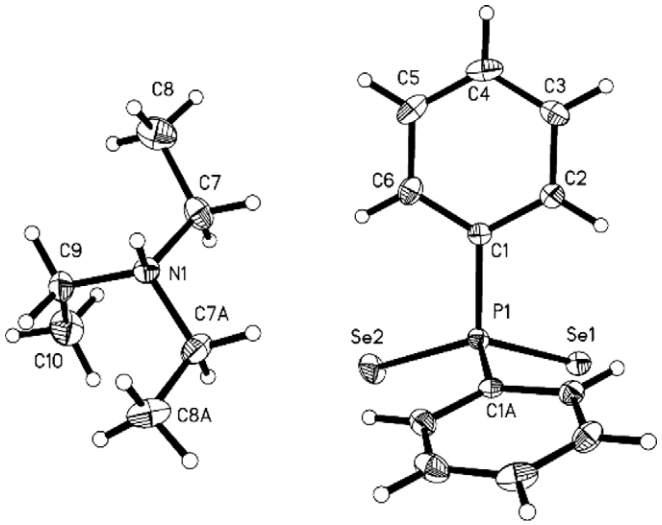

Fig. 3. Thermal ellipsoid plot (50% probability) of the structure of (**3**).

4. Growth of materials

4.1. Zinc selenide nanorods

The growth of ZnSe nanorods was carried by thermally decomposing $[Zn(^iPr_2PSe_2)_2]$ in HDA. HDA was used both as a solvent and a coordinating agent for the growth of nanorods. Fig. 5 shows the XRPD patterns of the ZnSe nanocrystals indicating characteristic line broadening pointed to the nanosized crystal domains. The XRPD peaks can be indexed by the wurtzite phased ZnSe (JCPDS 15-0105) with the strong characteristic (1 1 0), (1 0 3), (1 1 2) peaks (Table 3). The XRPD peaks indicates crystalline domain along the *c*-axis of the wurtzite lattice. The attribution was supported by the observation of an increasing intense and sharp (0 0 2) peak. It is interesting to find that there is no monomer effect on the crystal phase of ZnSe. All the samples are luminescent (Fig. 6). The peaks exhibit a blue shift with increase in concentration, reflecting the change in the optical bandgaps. The emission maximums are sample (a): 375 nm, sample (b): 414 nm, sample (c): 418 nm. The TEM studies indicate the formation of nanorods regardless of concentration of precursor. The average of rods using 0.4 g of precursor is 6.6 nm and the length is 24.1 nm (Fig. 7). The HR-TEM image of individual nanorods reveals regularly spaced lattice fringes with separation of 0.35 nm consistent with the spacing between the (1 0 0) lattice planes.

4.2. Antimony telluride thin films

The deposition of antimony telluride thin films were carried out using $Sb[(TeP^iPr_2)_2N]_3$ by aerosol-assisted chemical vapor deposition (AACVD) [40]. The precursor was synthesized according to the reported method [41]. A typical film deposition utilizes a solution of 0.10 g of the precursor dissolved in 10 ml toluene which was converted into aerosols using an ultrasonic humidifier [42]. The

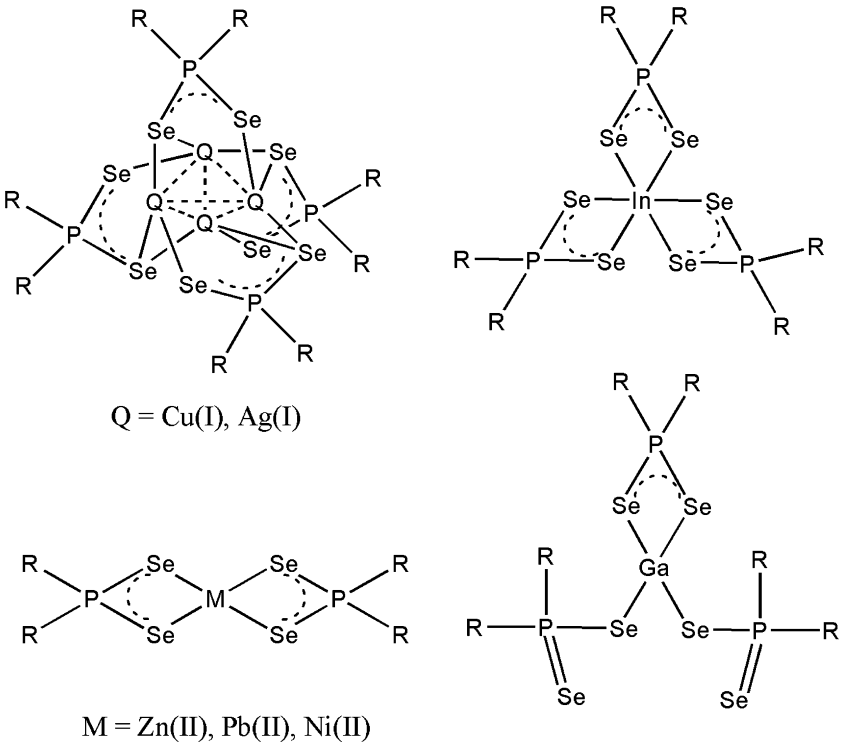

Fig. 4. Structures of metal dialkyldiselenophosphinates (R = ^{i}Pr, Ph, ^{t}Bu).

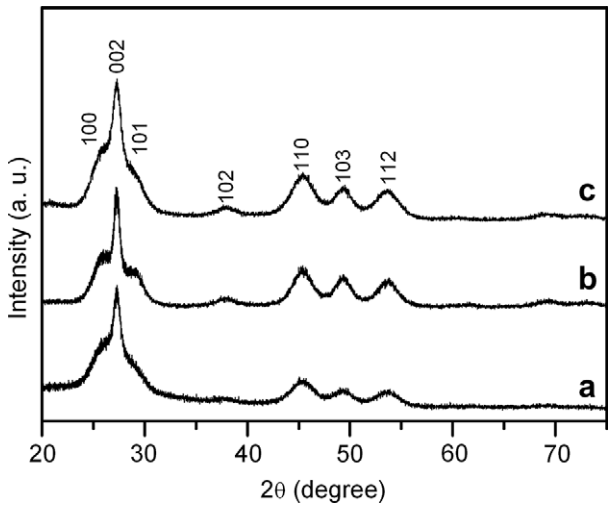

Fig. 5. XRPD patterns of hexagonal ZnSe (JCPDS 15-0105) nanoparticles synthesized at 300 °C from (a) 0.2 g; (b) 0.4 g and (c) 0.6 g of precursor for 30 min.

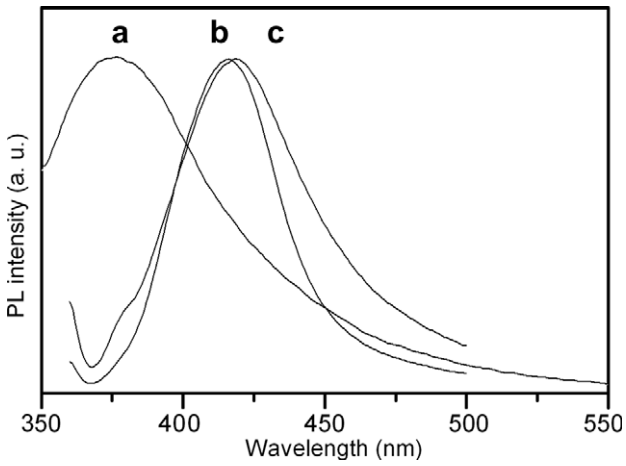

Fig. 6. Normalized PL spectra (excited at 340 nm) of ZnSe nanoparticles synthesized at different concentrations of precursor at 300 °C for 30 min: (a) 0.2 g; (b) 0.4 g, and (c) 0.6 g.

Table 3
Comparison of XRPD data for ZnSe nanoparticles

hkl	JCPDS (15-0105) *d* [Å] (rel. int.)	ZnSe (a) *d* [Å] (rel. int.)	ZnSe (b) *d* [Å] (rel. int.)	ZnSe (c) *d* [Å] (rel. int.)
100	3.43 (100)	3.42 (38)	3.42 (55)	3.42 (48)
002	3.25 (90)	3.25 (100)	3.38 (100)	3.26 (100)
101	3.05 (70)	3.05 (27)	3.05 (23)	3.04 (20)
102	2.36 (60)	2.38 (8)	2.37 (5)	2.36 (8)
110	1.99 (100)	2.00 (51)	2.00 (30)	2.00 (34)
103	1.84 (80)	1.84 (22)	1.85 (11)	1.85 (16)
112	1.70 (70)	1.71 (32)	1.70 (23)	1.71 (29)

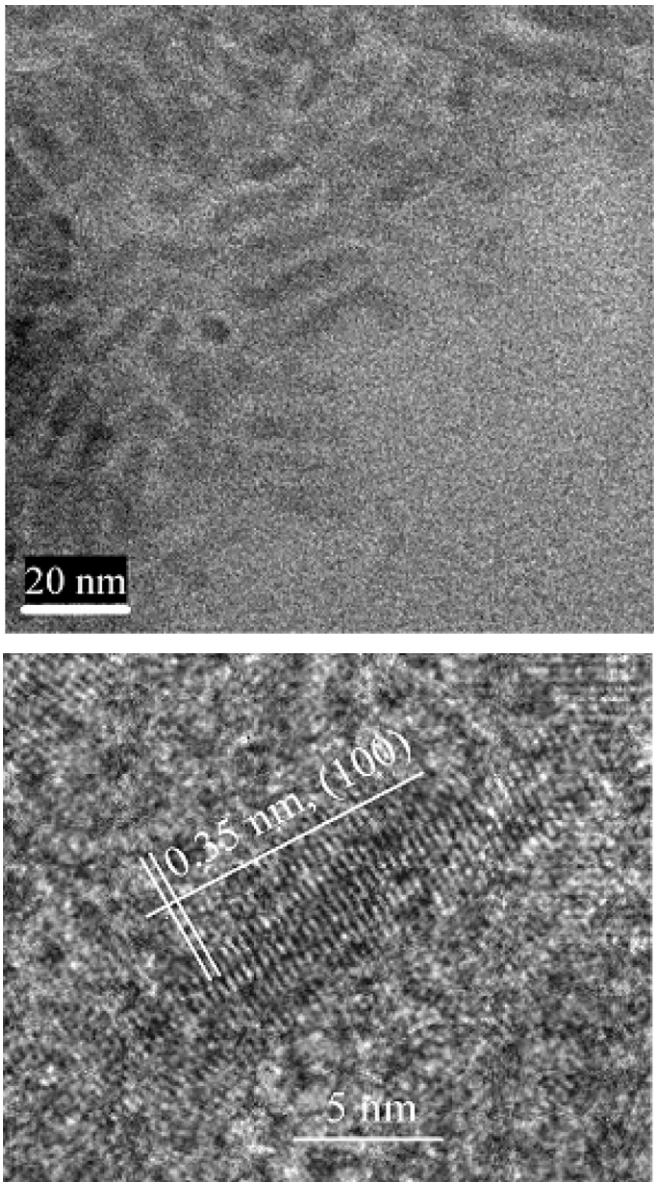

Fig. 7. A TEM image of ZnSe nanorods using 0.4 g of precursor obtained at 300 °C (top). A HR-TEM image of a single ZnSe nanorod is shown at the bottom.

Table 4
Comparison of XRPD data for Sb_2Te_3 nanoplates

hkl	JCPDS (15-0874) *d* [Å] (rel. int.)	Sb_2Te_3 *d* [Å] (rel. int.)
003	10.16 (2)	9.96 (100)
006	5.08 (4)	5.03 (49)
009	3.38 (6)	3.37 (9)
015	3.16 (100)	3.14 (11)
1010	2.35 (35)	2.33 (5)
110	2.13 (25)	2.10 (4)
0015	2.03 (4)	2.01 (6)
116	1.96 (2)	1.95 (6)
0018	1.69 (2)	1.68 (6)

deposition studies were carried out on glass substrates between 375 and 475 °C over 60 min. A substrate temperature of 325 °C was too low to initiate deposition. When the

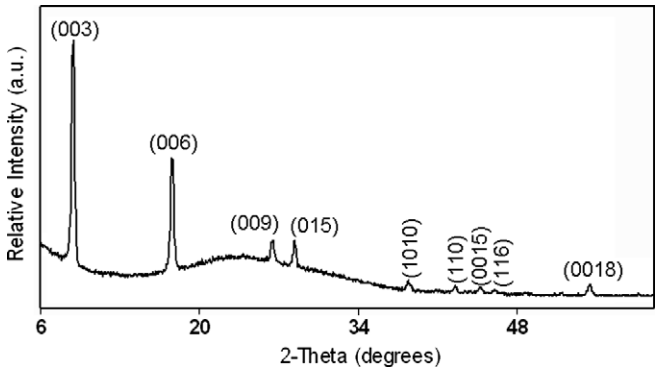

Fig. 8. A XRPD pattern of rhombohedral Sb_2Te_3 thin films deposited at 475 °C using a dynamic argon flow rate of 240 sccm.

growth temperature was increased to 375 and 475 °C, good quality black, reflective films were obtained on the glass substrates. The XRPD studies of as-deposited films exclusively showed the growth of rhombohedral Sb_2Te_3 with a space group of $R\bar{3}m$ (JCPDS: 15-0874) (Table 4). All the films have a preferred orientation along the (003) plane in the temperature range 375–475 °C (Fig. 8). The cell parameters for a rhombohedral unit cell were calculated and compared with the literature values (JCPDS: 15-0874). The calculated lattice values ($a = 4.257$ Å, $c = 30.373$ Å) are in good agreement with the reported values ($a = 4.264$ Å, $c = 30.458$ Å). The morphologies of the films were studied by SEM which clearly showed the formation of randomly orientated plates (Fig. 9). The deposition temperatures do not have profound effects on the film morphologies. The composition of the films was determined by EDAX from which the stoichiometry of films was found to be ca. 2:3.

Surface analysis of the films was carried out using X-ray photoelectron spectroscopy (Fig. 10). The Sb $3d_{5/2}$ and $3d_{3/2}$ peaks are observed at 529.7 and 537.3 eV, respectively. Additional peaks (525.9 and 535.4 eV) for Sb 3d indicate different chemical environments i.e., Sb–O and Sb–Te. The values of 539.6 eV ($3d_{3/2}$) and 530.3 eV ($3d_{5/2}$) are reported for antimony oxide in the literature [43]. A broad peak for Sb $3d_{3/2}$ is obtained due to overlapping with the O 1s (529.6 eV) peak. The two Te 3d signals, corresponding to Te–Sb and Te–O, are also seen. The values for Te–O, i.e., 584 eV ($3d_{3/2}$) and 574 eV ($3d_{5/2}$), are comparable to literature values of 586 ($3d_{3/2}$) and 576 eV ($3d_{5/2}$) [44]. The presence of the O1s peak indicates that oxidation of the film takes place after exposure to the atmosphere. A minor P $2p_3$ peak at 130.5 eV represents a possible decomposition product, which is present as a contaminant in the deposited films.

5. Conclusions

A new simple method is reported for the preparation of diselenophosphinate ligands which are perfectly air stable. The resulting zinc complex; $[Zn(^iPr_2PSe_2)_2]$ has been thermolysed in a capping ligand resulting in hexagonal

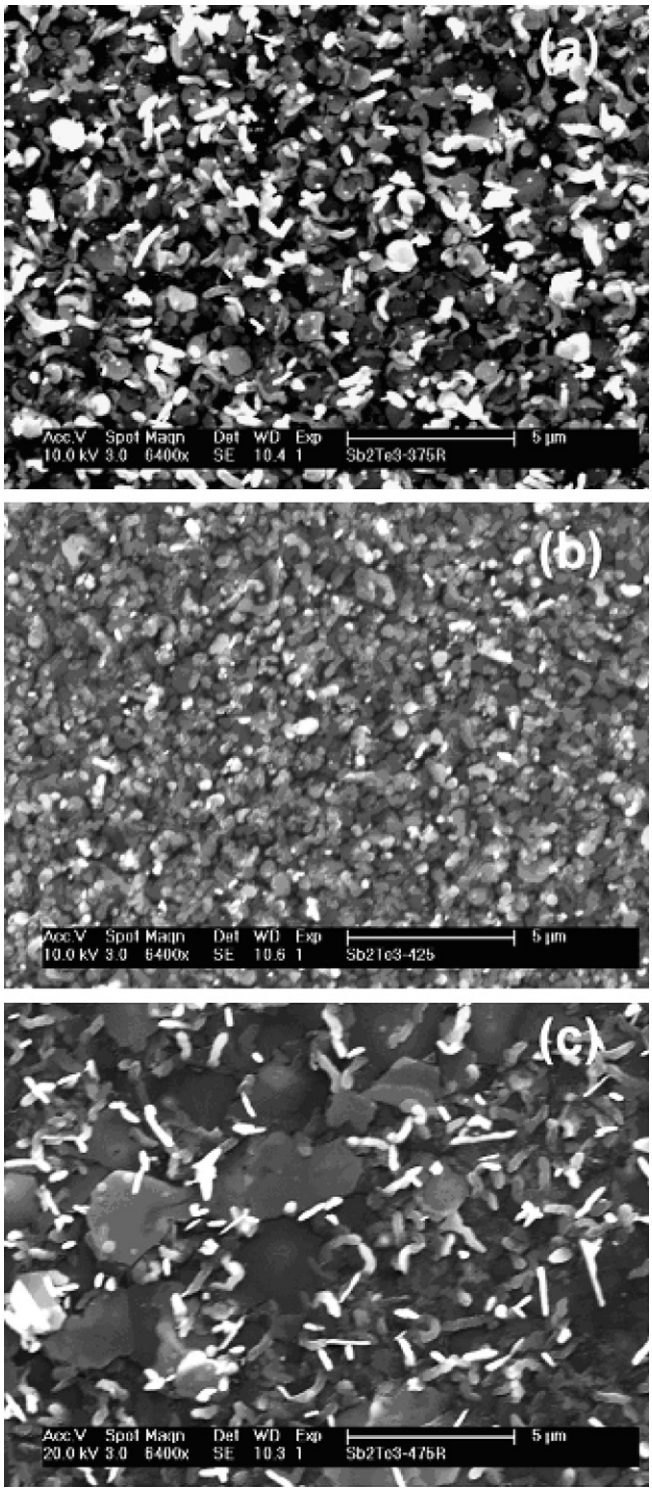

Fig. 9. SEM images of Sb_2Te_3 films deposited on glass at (a) 375 °C; (b) 425 °C and (c) 475 °C.

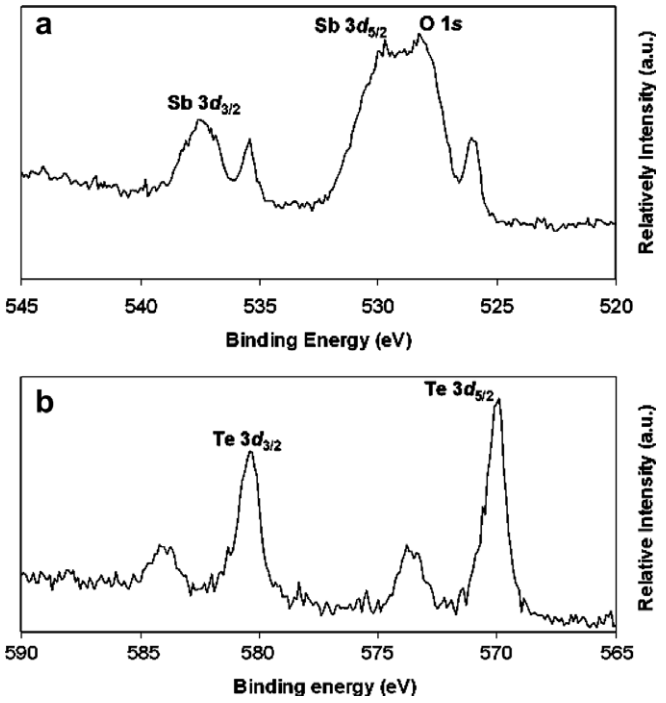

Fig. 10. Survey XPS scan for (a) Te and (b) Sb from the films grown at 475 °C.

ZnSe nanorods. A antimony telluride precursor based on ditelluroimidodiphosphinato ligand $[N(^iPr_2PTe)_2]^-$, has been used as a well-defined precursor to rhombohedral Sb_2Te_3 thin films by AACVD. Surface analysis of deposited thin films confirmed that the growth temperature do not have a profound effect on the morphologies of the deposited film, which are composed of hexagonal nanoplates.

Acknowledgements

We thank Prof. Tristram Chivers (University of Calgary, Calgary) for providing samples and Prof. Alice Sullivan (Queen Mary, University of London) and referees for useful discussions. The authors also acknowledge EPSRC (UK) for financial assistance. CQN acknowledge the funding from The Government of Vietnam.

Appendix A. Supplementary data

CCDC 291183, 291184 and 624157 contain the supplementary crystallographic data for this paper. These data can be obtained free of charge via http://www.ccdc.cam.ac.uk/conts/retrieving.html, or from the Cambridge Crystallographic Data Centre, 12 Union Road, Cambridge CB2 1EZ, UK; fax: (+44) 1223-336-033; or e-mail: deposit@ccdc.cam.ac.uk. Supplementary data associated with this article can be found, in the online version, at doi:10.1016/j.jorganchem.2006.11.043.

References

[1] B. Ludolph, M.A. Malik, P. O'Brien, N. Revaprasadu, Chem. Commun. (1998) 1849.
[2] N. Revaprasadu, M.A. Malik, P. O'Brien, M.M. Zulu, G. Wakefied, J. Mater. Chem. 8 (1998) 1885.

[3] (a) For example see; I. Haiduc, D. Sowerby, Polyhedron 15 (1995) 246;
(b) R.C. Mehrotra, G. Srivastava, B.P.S. Chauhan, Coord. Chem. Rev. 55 (1984) 207;
(c) B. Walther, Coord. Chem. Rev. 60 (1984) 67;
(d) I.J. Haiduc, Organomet. Chem. 623 (2001) 29;
(e) Y. Takahashi, R. Yuki, M. Sugiura, S. Motojima, K. Sugiyama, J. Cryst. Growth 50 (1980) 491;
(f) C. Byrom, M.A. Malik, P. O'Brien, A.J.P. White, D.J. Williams, Polyhedron 19 (2000) 211.
[4] (a) For example see; I.P. Gray, A.M.Z. Slawin, J.D. Woollins, Dalton Trans. (2005) 2188;
(b) C.W. Liu, T.S. Lobana, B.K. Santra, C.-M. Hung, H.-Y. Liu, B.-J. Liaw, J.-C. Wang, Dalton Trans. (2006) 560.
[5] (a) W. Kuchen, H. Hertel, Angew. Chem., Int. Ed. 8 (1969) 89;
(b) W. Kuchen, B. Knop, Angew. Chem., Int. Ed. 4 (1965) 244;
(c) W. Kuchen, J. Metten, A. Judat, Chem. Ber. 97 (1964) 2306;
(d) A. Müeller, V.V.K. Rao, P. Christophliemk, J. Inorg. Nucl. Chem. 36 (1974) 472;
(e) A. Müeller, V.V.K. Rao, P. Christophliemk, J. Inorg. Nucl. Chem. 34 (1972) 345;
(f) A. Müeller, V.V.K. Rao, P. Christophliemk, J. Inorg. Nucl. Chem. 104 (1971) 1905.
[6] M.J. Pilkington, A.M.Z. Slawin, D.J. Williams, J.D. Woollins, Polyhedron 10 (1991) 2641.
[7] P. Kilian, P. Bhattacharyya, A.M.Z. Slawin, J.D. Woollins, Euro. J. Inorg. Chem. (2003) 1461.
[8] R.P. Davies, M.G. Martinelli, Inorg. Chem. 41 (2002) 348.
[9] R.P. Davies, C.V. Francis, A.P.S. Jurd, M.G. Martinelli, A.J.P. White, D.J. Williams, Inorg. Chem. 43 (2004) 4802.
[10] C.Q. Nguyen, A. Adeogun, M. Afzaal, M.A. Malik, P. O'Brien, Chem. Commun. (2006) 2179.
[11] A. Schmidpeter, R. Böhm, M.H. Groeger, Angew. Chem. 76 (1964) 860.
[12] T.F. Wang, J. Najdzionek, K.L. Leneker, H. Wasserman, D.M. Braitsch, Synth. React. Inorg. Met.-Org. Chem. 8 (1978) 119.
[13] D. Cupertino, D.J. Birdsall, A.M.Z. Slawin, J.D. Woollins, Inorg. Chim. Acta 290 (1999) 1.
[14] D. Cupertino, R. Keyte, A.M.Z. Slawin, D.J. Williams, J.D. Woollins, Inorg. Chem. 35 (1996) 2695.
[15] D.J. Birdsall, A.M.Z. Slawin, J.D. Woollins, Polyhedron 20 (2001) 125.
[16] D.C. Cupertino, R.W. Keyte, A.M.Z. Slawin, J.D. Woollins, Polyhedron 18 (1999) 707.
[17] M. Necas, M.R.J. Foreman, J. Marek, J.D. Woollins, J. Novosad, New J. Chem. 25 (2001) 1256.
[18] I.P. Gray, A.M.Z. Slawin, J.D. Woollins, Dalton Trans. (2005) 2188.
[19] T.Q. Ly, J.D. Woollins, Coord. Chem. Rev. 176 (1998) 451.
[20] M. Afzaal, S.M. Aucott, D. Crouch, P. O'Brien, J.D. Woollins, J.H. Park, Chem. Vap. Depos. 8 (2002) 187.
[21] M. Afzaal, D. Crouch, M.A. Malik, M. Motevalli, P. O'Brien, J.-H. Park, J.D. Woollins, Eur. J. Inorg. Chem. (2004) 171.
[22] D.J. Crouch, P. O'Brien, M.A. Malik, P.J. Skabara, S.P. Wright, Chem. Commun. (2003) 1454.
[23] M. Afzaal, D.J. Crouch, P. O'Brien, J. Raftery, P.J. Skabara, A.J.P. White, D.J. Williams, J. Mater. Chem. 14 (2004) 233.
[24] M. Afzaal, S.M. Aucott, D. Crouch, P. O'Brien, J.D. Woollins, J.H. Park, Adv. Mater. 14 (2002) A187.
[25] P. Bhattacharyya, J.D. Woollins, Polyhedron 14 (1995) 3367.
[26] G.G. Briand, T. Chivers, M. Parvez, Angew. Chem., Int. Ed. 41 (2002) 3468.
[27] T. Chivers, D.J. Eisler, J.S. Ritch, H.M. Tuononen, Angew. Chem., Int. Ed. 44 (2005) 4953.
[28] J. Ellermann, M. Schutz, F.W. Heinemann, M. Moll, Z. Anorg. Allg. Chem. 624 (1998) 257.
[29] T. Chivers, D.J. Eisler, J.S. Ritch, Dalton Trans. (2005) 2675.
[30] C. Burda, X. Chen, R. Narayan, M.A. El-Sayed, Chem. Rev. 105 (2005) 1025.
[31] C.N.R. Rao, F.L. Deepak, G. Gundiah, A. Govindarj, Prog. Solid State Chem. 31 (2003) 5.
[32] (a) Z.X. Deng, C. Wang, X.M. Sun, Y.D. Li, Inorg. Chem. 41 (2002) 869;
(b) R. Solanki, J. Huo, J.L. Freeouf, B. Miner, Appl. Phys. Lett. 81 (2002) 3864;
(c) Y.C. Zhu, Y. Bando, Chem. Phys. Lett. 377 (2003) 367;
(d) J. Hu, Y. Bando, Z. Liu, T. Sekiguchi, D. Golderg, J. Zhan, J. Am. Chem. Soc. 125 (2003) 11306;
(e) X.T. Zhang, Z. Liu, K.M. Ip, Y.P. Leung, O. Li, S.K. Harka, Appl. Phys. Lett. 95 (2004) 5752;
(f) Y. Dong, Q. Peng, Y. Li, Inorg. Chem. Commun. 7 (2004) 370;
(g) C. Ye, X. Fang, Y. Wang, P. Yan, J. Zhao, L. Zhang, Appl. Phys. A 79 (2004) 113.
[33] C.A. Smith, H.W.H. Lee, V.J. Leppert, S.H. Rusbud, Appl. Phys. Lett. 75 (1999) 1688.
[34] (a) A.B. Panda, S. Acharya, S. Efrima, Adv. Mater. 17 (2005) 2471;
(b) A.B. Panda, G. Glaspell, M.S. El-Shall, J. Am. Chem. Soc. 128 (2006) 2790.
[35] M.A. Malik, N. Revaprasadu, P. O'Brien, Chem. Mater. 13 (2001) 913.
[36] S.L. Cumberland, K.M. Hanif, A. Javier, G.A. Khitrov, G.F. Strouse, S.M. Woessner, C.S. Yun, Chem. Mater. 14 (2002) 1576.
[37] G.M. Sheldrick, SHELXL97 and SHELXS 97, University of Göttingen, 1997.
[38] Bruker, SHELXTL. Version 6.10, Bruker AXS Inc., 2000.
[39] C.Q. Nguyen, M. Afzaal, M.A. Malik, P. O'Brien, unpublished results.
[40] S.S. Garje, D.J. Eisler, J.S. Ritch, M. Afzaal, P. O'Brien, T. Chivers, J. Am. Chem. Soc. 128 (2006) 3120.
[41] T. Chivers, D.J. Eisler, J.S. Ritch, Dalton Trans. (2005) 2675.
[42] G.A. Horley, M.R. Lazell, P. O'Brien, Chem. Vap. Depos. 2 (1996) 242.
[43] F. Garbassi, Surf. Interface Anal. 2 (1980) 165.
[44] H.-Y. Cheng, C.A. Jong, R.-J. Chung, T.S. Chin, R.-T. Huang, Semicond. Sci. Technol. 20 (2005) 1111.